High-temperature extensional rheology of linear, branched, and hyper-branched polycarbonates

Article *in* Rheologica Acta · June 2019

DOI: 10.1007/s00397-019-01157-9

3 authors, including:

Samrat Sur
University of Massachusetts Amherst
3 PUBLICATIONS **4** CITATIONS
SEE PROFILE

Manojkumar Chellamuthu
Saudi Basic Industries Corporation (SABIC)
5 PUBLICATIONS **121** CITATIONS
SEE PROFILE

Rheologica Acta
https://doi.org/10.1007/s00397-019-01157-9

ORIGINAL CONTRIBUTION

High-temperature extensional rheology of linear, branched, and hyper-branched polycarbonates

Samrat Sur[1] · Manojkumar Chellamuthu[2] · Jonathan Rothstein[1]

Received: 2 August 2018 / Revised: 12 March 2019 / Accepted: 5 June 2019

Abstract

The high-temperature extensional viscosity of three commercially available linear, branched and hyper-branched polycarbonates (PCs) were measured using a high-temperature capillary breakup extensional rheometer (CaBER) in both air and nitrogen. The experiments were performed at temperatures ranging from $T = 250$ to 370 °C to a maximum Hencky strain of ten. At lower end of the temperature range, no significant degradation of the linear and branched PC was observed either in the shear or extensional measurements. Beyond, $T > 300$ °C degradation of the three different PCs was observed. Changes to the molecular structure of the PC were observed which resulted in a dramatic increase in the extensional viscosity. The rate of growth in the extensional viscosity was found to increase with temperature, time at temperature, and, in the case of the linear and branched PC, the presence of air. For the hyper-branched case, changes to the molecular structure of the PC were found to occur more quickly under nitrogen. At these high temperatures, the increase in extensional viscosity was found to grow large enough to stop the breakup of the fluid filament all together, essentially stopping all capillary drainage. This temperature-induced cross-linking and increase in the extensional viscosity of the PC can improve the anti-dripping properties of the polycarbonate by slowing and even restricting dripping from polymeric components near high heat surges. Through these experiments, we have demonstrated measurement of the extensional viscosity to be several orders of magnitude more sensitive to temperature-induced changes to the molecular structure than measurements of shear rheology.

Keywords Polymer melt · Uniaxial extension · Shear rheology · Cross-linking · Melt dripping · Polycarbonate

Introduction

Polycarbonate (PC) is a widely used engineering polymer and with excellent mechanical properties, dimensional stability, heat resistance, and transparency. Since its introduction in the late 1950s, the use of bisphenol-A polycarbonate has grown steadily. Over the years, a variety of new uses for PC has been created by tailoring the base polycarbonate polymer with modification that enhances its end-use properties. One main approach is to modify the backbone of the polycarbonate. As with most polymers, polycarbonate can be formulated with linear, branched, and hyper-branched backbone architecture. Each of these polymer architectures shows different rheological behaviors and solid-state properties. As an example, branched polymers are often used for the applications characterized by strong extensional flow fields in the molten state such as extrusion coating, blow molding, foam extrusion, and melt phase thermoforming because addition of branching is known to enhance the extensional viscosity of polymer melts (DeMaio et al. 2000).

In many applications, polymer materials can be exposed to high temperatures either intentionally or unintentionally. Unfortunately, polymers are highly flammable, with combustion most often accompanied by the production of corrosive or toxic gases and smoke. Consequently, improving the fire-retardant behavior of polymers has become a major challenge

Electronic supplementary material The online version of this article (https://doi.org/10.1007/s00397-019-01157-9) contains supplementary material, which is available to authorized users.

✉ Jonathan Rothstein
rothstein@ecs.umass.edu

Samrat Sur
ssur@umass.edu

Manojkumar Chellamuthu
Manojkumar.chellamuthu@sabic.com

[1] Department of Mechanical and Industrial Engineering, University of Massachusetts, Amherst, MA 01003, USA

[2] SABIC, Mt. Vernon, IN 47620, USA

Published online: 21 June 2019

for extending their use to a wide array of commercial applications. The scientific and technical literature contains a very diverse array of strategies for improving polymer fire resistance. These strategies depend primarily on the nature and chemical structure of the polymer concerned, its decomposition mode, the required level of fire safety, and the global performances of the resulting materials (Laoutid et al. 2009). The development of flame-retardant materials and the understanding of the phenomena that take place during combustion often require close collaboration between several fields of scientific expertise including: macromolecular and physical chemistry, physics of mass transfer and heat transfer, and rheology.

The most common chemical changes that can take place during thermal decomposition of polymers include the following: random chain scission, in which the polymer chain is cleaved at random locations along its backbone; end chain scission, in which individual monomer units are successively removed at the chain end; chain stripping, in which side groups or atoms are cleaved; and cross-linking, in which bonds are created between polymer chains (Beyler and Hirschler 2002). All these changes can be detected through rheological measurements. The first three changes involve chain scission, which will reduce the viscosity of the polymer melt making the polymers more likely to drip and feed a fire from above, while cross-linking will increase both the shear and the extensional viscosity of the melt making the polymer less likely to drip. It is the likelihood of dripping, which is one of the primary ways that a polymeric material's flame resistance is classified and its suitability for use in many commercial applications is established.

In order to better understand the process of drop formation that can feed a flame and negatively affect a material's flame resistance, one must consider the dynamics of dripping and the formation of droplets (Clasen et al. 2012; McKinley 2005; Rayleigh 1879; Stone 1994). For high viscosity liquids, like the polymer melts studied here, the Ohnesorge number is greater than one and dripping is resisted by viscous forces with a characteristic time for breakup that scales with the viscous timescale, $\tau_v = \eta R_0/\sigma$. Here, σ is the surface tension, R_0 is the initial drip radius, and η is the shear viscosity of the fluid. It is important to note, however, that during breakup, the drainage of the polymeric fluid into the primary drops is a purely extensional flow. For polymers, which are viscoelastic fluids, it is thus the extensional viscosity, η_E, and not the shear viscosity that controls the viscoelastic breakup time, $\tau_{VE} = \eta_E R_0/\sigma$ (Mun et al. 1998; Renardy 1995). As the extensional viscosity and the time between drips increases for these viscoelastic fluids, the time the polymer is exposed to a high-temperature heat source increases along with the time available to undergo thermal decomposition. Thus, understanding the extensional rheology of a polymer under extreme conditions is an important step towards being able to predict the response of a polymer when exposed to a flame.

A number of recent papers have tried to quantify the dripping behavior of polymers exposed to flames or simply at elevated temperatures. Most studies have been performed under fire operating conditions that resemble the industry standard UL 94 test which exposes a polymer sheet to an open flame under very specific conditions to determine whether or not the polymer will drip (Wang et al. 2012; Wang et al. 2010). A number of recent studies have tried to understand the dripping in a more systematic and controlled way (Kandola et al. 2014; Kandola et al. 2013; Matzen et al. 2015). Kandola et al. (2013) developed an electric furnace and the polymers were exposed to convective heating at a constant elevated temperature. The number, diameters, and shapes of individual drops were measured and found to be influenced by the mechanism of decomposition of each polymer type. They were able to quantify the melt-dripping tendency of thermoplastic polymers under different conditions and relate them to their mechanisms of decomposition. Similarly, Matzen et al. (2015) used a similar heating furnace to look at the effect of adding flame retardant on the melt dripping behavior of various commercially available polymers such as polypropylene (PP), polybutylene terephthalate (PBT), and polyamide (PA). They experimentally monitored the mass loss due to melt dripping, drop size, and drop temperature as a function of the furnace temperature applied to a rod-shaped polymer specimen. They found that while some flame-retardant additives promoted melt dripping, others were effective at arrested melt dripping and improving flame retardance. Matzen et al. (2015) also showed that the shear viscosity of the polymer was a major influence in melt dripping and that a direct correlation between the melt dripping and zero shear rate viscosity at steady flow conditions could be made. However, even though shear viscosity variation with temperature is useful in understanding, and in some cases even predicting dripping behavior, because dripping is a purely extensional flow, we hypothesize that characterization of the variation of extensional viscosity with temperature should be far better at predicting whether a polymer will drip when exposed to a flame. However, to date, no paper has investigated the quantitative relationship between the extensional rheology of thermoplastics and their melting dripping behavior at elevated temperatures where chemical changes to the backbone are expected.

In this paper, we will demonstrate how uniaxial extensional rheology measurement can be used as a method for characterizing the performance of polycarbonates (PC) of different molecular structure (linear, branched, and hyper-branched) at high temperatures where degradation is expected similar to what occurs when a sample is exposed to a flame. The extensional rheology measurements presented in this paper were performed using the capillary breakup extensional rheometry (CaBER). Using CaBER, the time evolution of the extensional viscosity of linear, branched, and hyper-branched PC was systematically explored performed both in air and in an inert

nitrogen environment. Through our study, we will show that measurements of extensional viscosity are far more sensitive to changes in the molecular architecture of the polymer than measurements of shear viscosity. We will show that cross-linking of the polymer chains at high temperature can lead to divergence in the extensional viscosity and the eventual cessation of dripping. And finally, we will show that the flame resistance of these polycarbonate samples can be directly classified based on the evolution of their extensional viscosities at extremely high temperatures.

Experimental setup

Materials

High-temperature extensional rheology measurements were performed on a series of commercially available polycarbonates. These included a linear PC (Lexan 130, a branched PC (Lexan), and a hyper-branched PC. The material was generously provided by SABIC in the form of pellets. The linear polycarbonate PC had a molecular weight of M_w = 36 kg/mol with a PDI of 1.74. The branched polycarbonate had a molecular weight of M_w = 36 kg/mol with a PDI of 1.88 and contained the branching agent 1,1,1-Tris hydroxy phenyl ethane (THPE). The hyper-branched had a molecular weight of M_w = 28 kg/mol with the end group hydroxy benzoyl nitrile (HBN) and PDI of 3.15. Before being tested in shear and extensional rheometers, the pellets were first molded to fit the plate geometry in the hot press under vacuum at T = 250 ° C.

Thermal analysis

Thermal properties of all the samples were measured by thermo-gravimetric analysis using (TA-Q50) under nitrogen and air at a heating rate of 10 ° C/min from T = 30 to 900 ° C. In nitrogen, the mass loss, which is a sign of degradation, began at a temperature of T = 450 ° C for the linear PC, T = 425 ° C for the branched PC, and T = 400 ° C for the hyper-branched PC. In comparison to mass loss in nitrogen, mass loss in air consistently started about 20 ° C earlier for each polymer. The residue was found to remain constant in nitrogen beyond T = 600 ° C, but the residue continued to decrease in air and eventually went to zero. From DSC measurements (TA-Q100), the glass transition temperatures, T_g, was found to be T_g = 140 ° C for the hyper-branched, T_g = 150 ° C for the linear, and T_g = 151 ° C for the branched PC.

Capillary breakup extensional rheometry

Capillary breakup extensional rheometer (CaBER) was chosen for these experiments because the dynamics of filament decay during a CaBER experiment closely match those experienced during dripping. In addition, measurements of extensional viscosity with CaBER are in many ways optimized for these high-temperature environments as they require a small, easily heated oven with optical access to observe filament decay with time. Conversely, other rheological techniques like Filament Stretching Extensional Rheometry (FiSER) require a large, tall oven to accommodate several meters of stretch.

Due to natural convection, the temperature in such an oven can be challenging to maintain (Bach et al. 2003; Bischoff White and Rothstein 2012; Chellamuthu et al. 2011). Additionally, FiSER requires a load cell to measure force on the plate that is exposed either directly or indirectly to an extremely high-temperature environment (Bach et al. 2003; Bischoff White and Rothstein 2012; Chellamuthu et al. 2011). Finally, both CaBER measurements and the dripping of a polymer exposed to fire are driven by capillary breakup and, as such, the kinematics of the process and the amount of the polymer melt interface exposed to heat and the environment are quite similar making conclusions on dripping more easily drawn from CaBER experiments than FiSER or shear rheology measurements. A schematic diagram of the CaBER with its main components is shown in Fig. 1. Here, we have customized it for high-temperature measurements by building an oven around it that can reach up to 400 ° C using three 250-W resistance heaters (Omega-WS series). The oven temperature is controlled using a PID temperature controller (Omega-CN-2110) with a temperature accuracy of ±2 ° C. The oven is made of an inner and outer box fabricated from steel plates with insulation between the two boxes to reduce heat transfer out of the oven. The thickness of insulator was designed to maintain an inside temperature of T = 400 ° C without exceeding an outside oven surface temperature of 35 °C. A thickness of 6.25 cm of a silica-based insulator (Microsil, Zircar) with a thermal conductivity of k = 0.024 W/mK was used to maintain the outside temperature below 35 °C. Rectangular openings were cut into the sides of both the inner and outer box and covered with an inner and outer window made of Pyrex glass to allow optical access for the camera to allow for visualization of the filament diameter so that it could be measured optically as a function of time. The diameter measurements had a resolution of 6.3 μm/pixel based on the maximum magnification of the lens and the pixelation of the camera sensor. Provisions were made for supplying nitrogen and air into the oven so that measurements could be made in an inert or an oxygen-rich environment. The top plate was connected to a liner motor (LinMot-C1250) using a glass mica rod to reduce heat flow out of the oven and minimize the risk of heat damages to the motor. The motor was capable of stretching the fluid at speeds up to 200 mm/s. An edge detection software (Edgehog) was used to capture the diameter decay with time with subpixel resolution. In order to calculate the extensional viscosity, the diameter decay was fit with a spline and then differentiated.

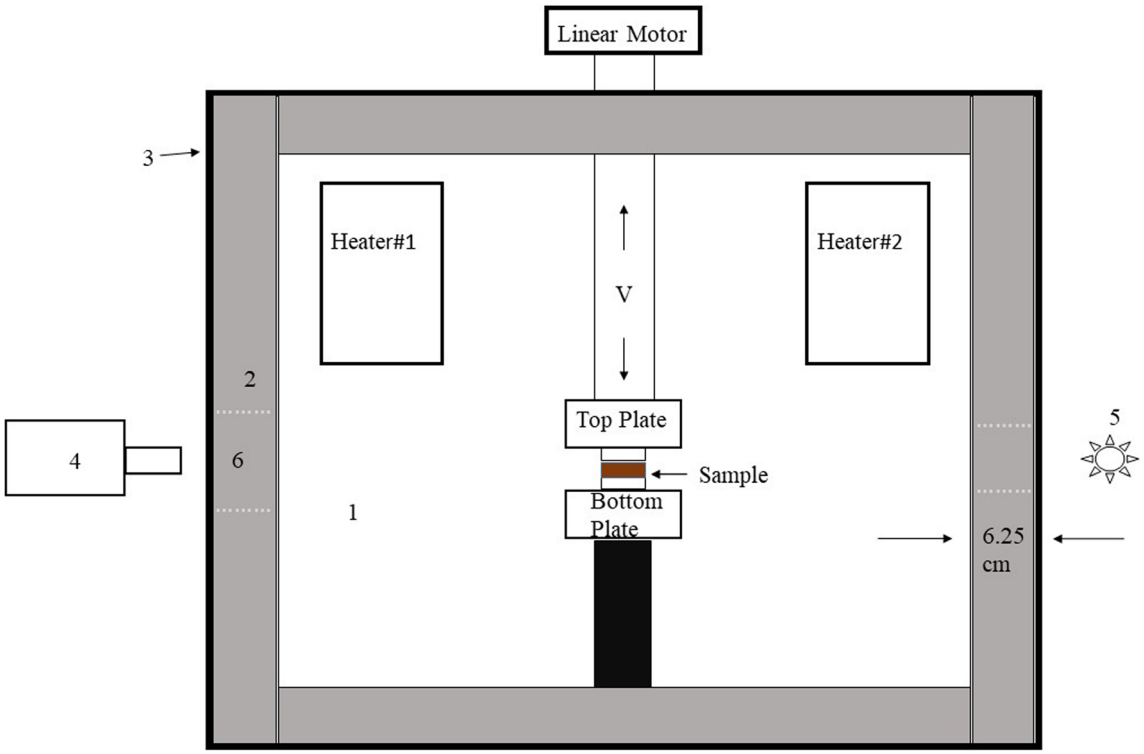

Fig. 1 Front view of the high-temperature extensional rheometer. The figure includes (1) inner box with the heaters, top plate, and the bottom plate, (2) heat shield (silica-based insulation) of thickness 6.25 cm on all sides, (3) outer box with the motor mounted on top, (4) camera for visualizing the stretch, (5) light source, and (6) windows for filament observation

Capillary breakup extensional rheometry measurements have become an increasingly common technique for determining the extensional rheology of viscoelastic fluids (Anna and McKinley 2001; Bazilevsky et al. 1990; Clasen et al. 2006; Entov and Hinch 1997; Kojic et al. 2006; McKinley and Tripathi 2000; Plog et al. 2005; Rodd et al. 2005; Stelter et al. 2000; Yesilata et al. 2006). In the CaBER experiments presented here, a cylindrical sample which had been melt cast using a hot press under vacuum was placed between two cylindrical plates at room. The oven was then turned on and heated to the desired experimental temperature with a ramp of 5 °C/min. Once the desired temperature was reached, the sample was then stretched with the top plate moving at a velocity of 0.01m/s until a gap of $3L_0 = 6.75$ mm was reached. Here, $L_0 = 2.25$ mm is the initial starting gap between the plates and $R_0 = 2.25$ mm is the initial radius of the sample melt. The stretch was then stopped and the capillary thinning of the liquid bridge that was formed between the two endplates subsequently produced a uniaxial extensional flow from which the extensional viscosity and relaxation time of the test fluid could be measured. A schematic diagram of the stretch is shown in Fig. 2.

In order to calculate the apparent extensional viscosity of a fluid undergoing a visco-capillary decay, like those observed here, the diameter measurements as a function of time were first fit with a spline to smooth the data and then differentiated before substituting into Eq. 1 (Papageorgiou 1995). The value of the surface tension was taken from the literature to be $\sigma =$ 34.2 mN/m.

$$\eta_E = -\frac{0.213\sigma}{dR_{mid}/dt}. \quad (1)$$

Results and discussions

Shear rheology

Small amplitude oscillatory and steady shear measurements were carried out using a controlled-stress rheometer (TA Instruments, ARES-G2). A parallel plate geometry with a 25 mm diameter and a 1.5 mm gap was employed at temperatures between $T = 160$ and 300 °C. A plot of storage modulus, G', and loss modulus, G'', ranging over eight decades of frequency covering the response from the terminal regime to glassy regime is presented in Fig. 3 utilizing time-temperature superposition. For the linear PC, a typical rheological response was observed exhibiting the expected terminal regime behavior with storage modulus varying as $G' \propto \omega^2$ and loss modulus proportional to $G'' \propto \omega$ in the lower the frequency range. The shift factors presented in Supplemental Figure S1, were not valid beyond $T = 300$ ° C because degradation of the

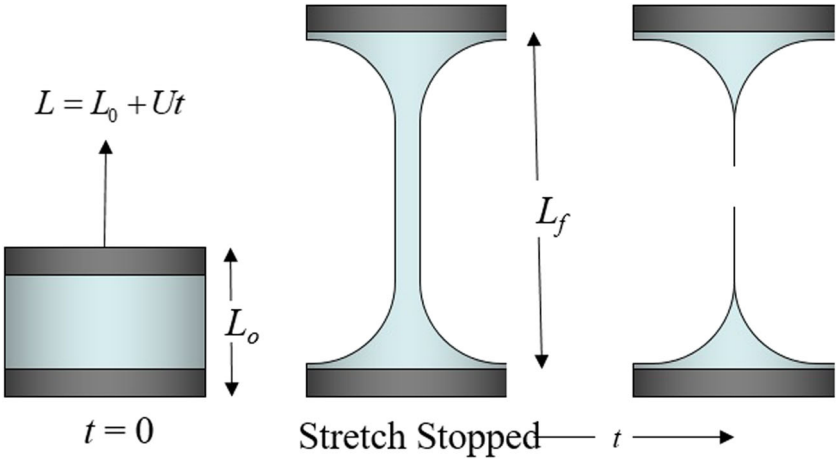

Fig. 2 Schematic diagram of capillary breakup extensional rheometry (CaBER)

PC was found to lead to time-dependent rheology. The cross-over point, which is the point of intersection of the G' and G'', can be used to estimate the relaxation time of the fluid. Although it is quite clear for the linear PC, it becomes less distinct as the degree of branching was increased. This is likely due to long relaxation time associated with the branch points and the polydispersity of the molecular weight of the branches. Reptation is the main relaxation method for linear polymers whereas branched chains relax by arm retraction. Research has shown that this leads to a retardation of chain movement along its backbone and, consequently, a broadening of the relaxation spectrum which can be seen in the broad shoulder observed in the G', G'' data (He et al. 2004).

In Fig. 4, a plot of complex viscosity, η^*, is shown as a function of angular frequency, ω, at a temperature of $T =$ 300 °C for linear, branched, and hyper-branched PC. From the literature (Kulicke and Kniewske 1984), we know that the zero-shear-rate viscosity for a linear PC scales with molecular weight as $\eta_0 \propto M_w^{3.4}$. This dependence on molecular weight increases as the level of branching increases which can be observed from the plot where branched PC has a higher complex viscosity as compared to linear PC at lower frequencies even though they are of the same molecular weight. Also from Fig. 4, a rapid shear thinning for hyper-branched and branched PC as compared to linear PC can be observed which is due to the presence of long relaxation time related to branched chains. Similar results have been seen in literature (Najafi et al. 2014). From Figs. 3 and 4, the relaxation time of the three sample can be approximated in a number of ways. Here, we fit a line through the Newtonian region and through the power law region and taking the inverse of the frequency ω at which it intersects to be the relaxation time. Using the above

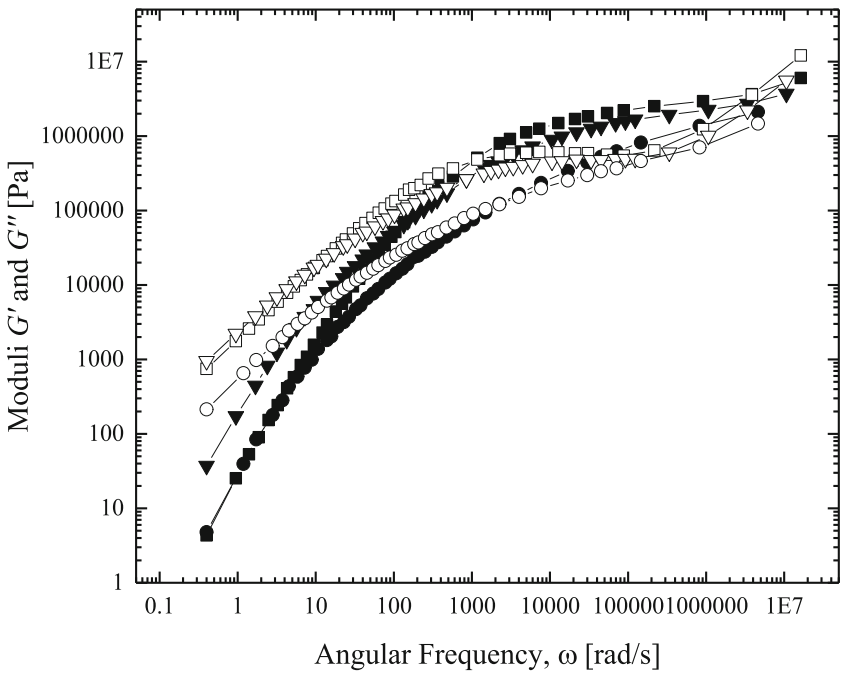

Fig. 3 Small amplitude oscillatory shear measurements of the storage and loss moduli (G' and G'') as a function of applied angular frequency for three different polycarbonates: linear PC (black square), branched PC (black down-pointing triangle), and hyper-branched PC (black circle). Filled symbols correspond to G' while hollow symbols correspond to G''. Data was taken at temperatures between $160\,° \leq T \leq 300°$ and shifted to a temperature of $T = 300\,°\,C$

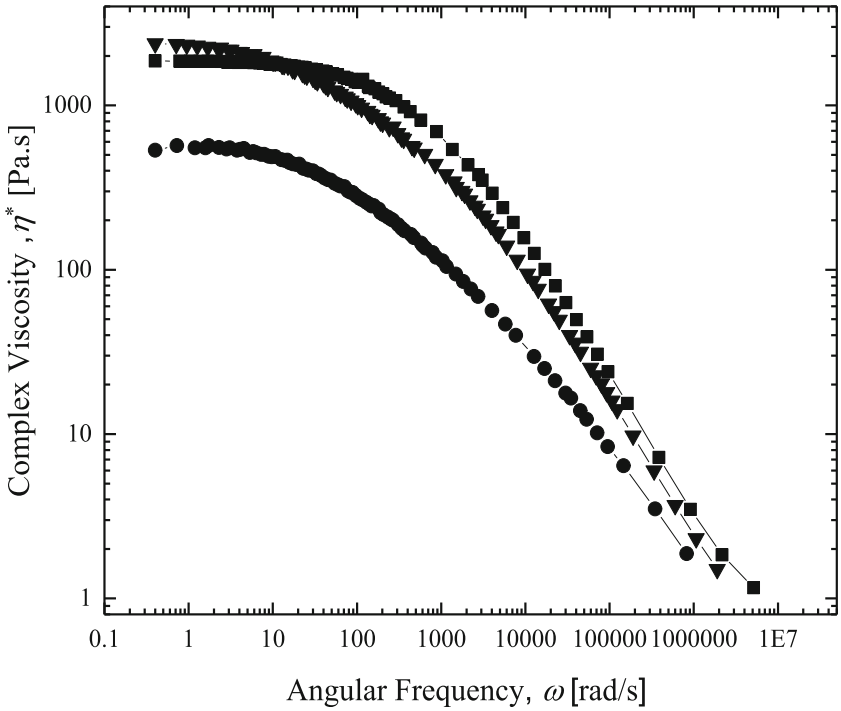

Fig. 4 Complex viscosity, η^*, as a function of angular frequency, ω, for the linear (black square), branched (black down-pointing triangle), and hyper-branched PC (black circle) at a temperature of $T = 300$ °C

fitting method, the calculated relaxation time for linear PC is $\lambda = 0.0025$ s, for branched PC $\lambda = 0.005$ s, and for hyper-branched PC $\lambda = 0.01$ s at $T = 300$ ° C. This relaxation time can be shifted to lower temperature range using the time-temperature superposition shift factors.

A series of time-resolved rheometry measurements were performed on all three samples at $T = 340$ °C. These measurements were performed at several frequencies between $\omega =$ 1 rad/s and $\omega = 100$ rad/s to look for the critical gel point of these material which indicates the transition from a viscoelastic liquid to a soft solid. The frequencies were chosen to be as large as possible so that the change in polymer properties could be minimized during each measurement point. The results are shown in Fig. 5 as the normalized loss tangent, $2\delta/\pi$. Similar experimental protocols have been used in the literature to study thermo-oxidative degradation of polyethylene terephthalate (Kruse and Wagner 2016) and also polyamide 11 (Filippone et al. 2015). For the linear and branched PC in air, a crossover of all the normalized loss tangents tested is observed at $t = 1600$ s and 1200 s, while no crossover was observed under nitrogen as shown in Supplementary Figure S2. This crossover, where the loss tangent becomes independent of frequency, is known as the critical gelation point. Winter and Chambon (Winter and Chambon 1986) showed that at the critical gel point, the material transitions from a liquid phase to a solid phase. In Fig. 5, the presence of this critical gel point clearly demonstrates that the linear and branched PC are undergoing a cross-linking reaction under air at $T = 340$ ° C. For the case of hyper-branched PC, the gel point was observed both in the presence of air and nitrogen at a time of $t = 700$ s and 1600 s respectively. The cross-linking reaction clearly occurs much faster in air. However, the fact that the hyper-branched PC cross-links at all in nitrogen while the linear and branched do not might be due to the presence of an end group which promoted both branching and cross-linking reactions even in the presence of nitrogen.

Although the loss tangent is an effective way to determine the critical gel point, perhaps a more intuitive way to understand the changes that are occurring the polymers at these extreme temperatures is to present the storage modulus as a function of time. In Fig. 6, the storage modulus, G', as a function of time for the linear and the branched PC at frequency of $\omega = 10$ rad/s and at temperatures of $T = 320$ ° C, $T = 340$ ° C, and $T = 360$ ° C in the presence of air. At $T = 320$ ° Cand $T = 340$ ° C, the storage modulus of the linear PC was found to show very little variation with time, whereas, for branched PC and hyper-branched PC at $T = 340$ ° C, the storage modulus was found to increase by a factor of two and three over time due to molecular structure buildup which takes place at that temperature respectively. As the temperature was increased to $T = 360$ ° C, an increase in the storage modulus was observed for all the three samples as shown in Fig. 6b. For the case of linear PC and branched PC, an increase in the storage modulus by a factor of 15 was observed whereas for the case of hyper-branched PC, an increase by a factor of 45 was observed. This rapid increase in storage modulus is due to the rapid buildup of molecular structure which has also been observed in the works of (Salehiyan et al. 2017). Similar trend in storage modulus, G', was observed in the works of Shangguan et al. (Shangguan et al. 2010). By using the term molecular structure buildup, we are hypothesizing that the increase in elastic modulus is a direct result of creation of

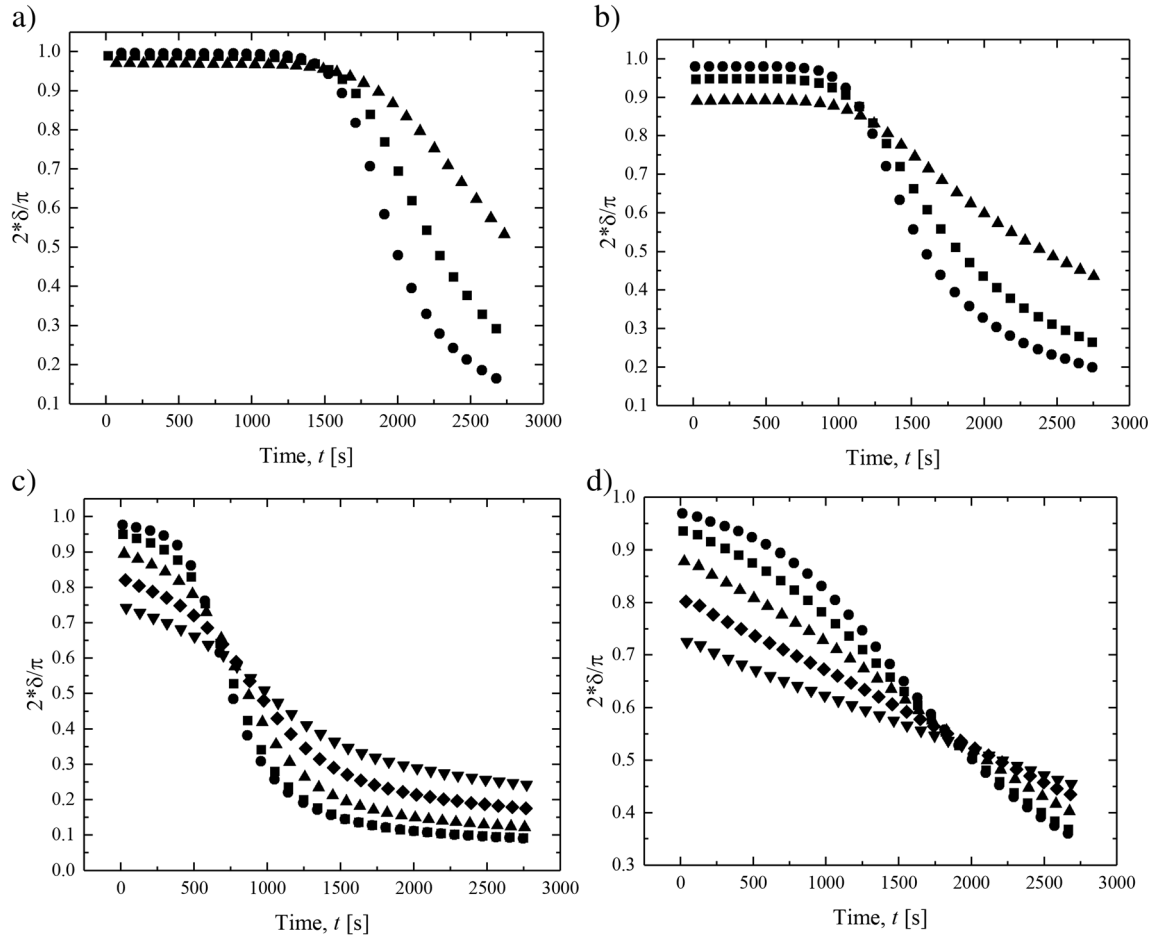

Fig. 5 Time resolved rheometry of loss tangent for **a** linear PC, **b** branched PC, **c** hyper-branched PC at 340 °C in the presence of air, and **d** hyper-branched PC in the presence of nitrogen at frequency of (black down-pointing triangle) $\omega = 100$ rad/s, (black diamond suit) $\omega = 31.6$ rad/s, (black up-pointing triangle) $\omega = 10$ rad/s, (black square) $\omega = 3$ rad/s, and (black circle) $\omega = 1$ rad/s

additional short or long branches along the polymer backbone or the cross-linking of adjacent polymeric chains together to build up an interconnected elastic network structure over time. Either would result in an increase in the storage modulus and are difficult to

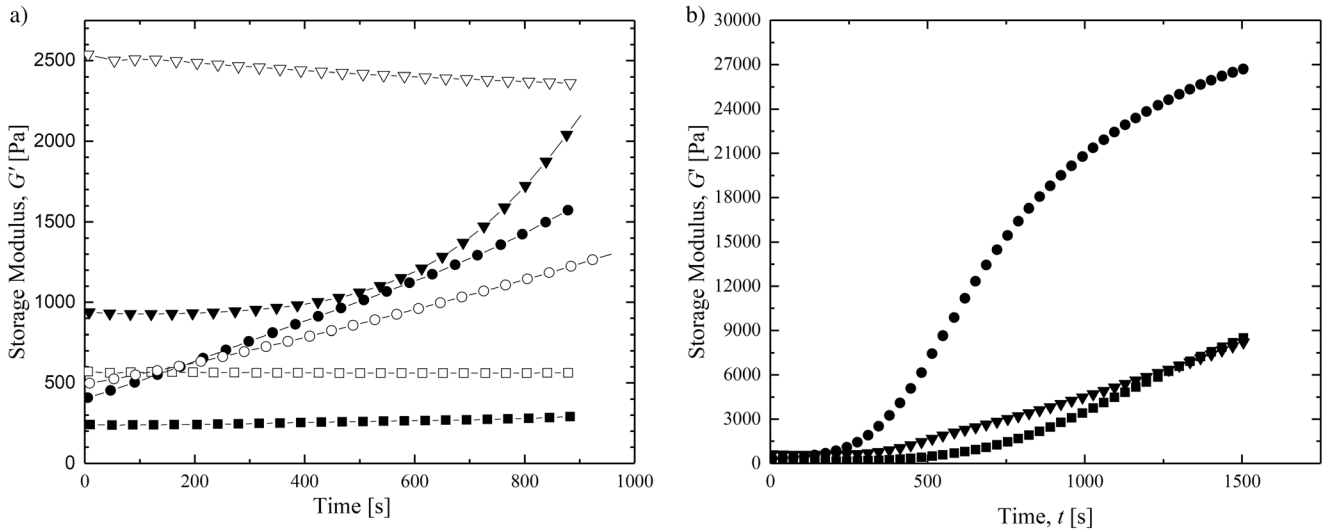

Fig. 6 Storage modulus, G', of linear (white square) branched (white down-pointing triangle), and hyper-branched (white circle) PC as a function of time t at a frequency of $\omega = 10$ rad/s in air at temperatures of **a** $T = 320$ °C (hollow symbols) and $T = 340$ °C (filled symbols) and **b** at $T = 360$ °C

distinguish in the DSC, TGA measurements that were performed after the experiments and will be described in detail later in the text. In Shangguan et al. (2010), they concluded that the increase in storage modulus is attributed to cross-link reaction and that oxidative degradation and cross-linking are the main reasons for the rheological changes observed in the polymer melt.

The maximum increase in storage modulus over time was seen for hyper-branched PC at $T = 360\,^{\circ}$C. In that case, an increase by a factor of 45 over the same period was observed which was likely due to the presence of the additional end groups available for cross-linking or perhaps residual catalyst in the resin. Similar measurements were performed in the presence of nitrogen. Unlike in the case of air, for the linear and branched PC, no increase in storage modulus was observed over the period of experiment. Thus, the polymer was found to be thermally stable in the presence of nitrogen at $T = 320$ °C and $T = 360$ °C. Although, at $T = 360$ °C, the storage modulus during the experiment was found to be lower as compared to that at $T = 320$ °C. This was due to the effect of time temperature superposition. Whereas, for the case of hyper-branched case, an increase in the storage modulus was observed in the presence of nitrogen at $T = 320$ °C and at $T = 360$ °C over the period of experiment. Thus, hyper-branched PC was found to be thermally less stable due to the presence of an end group as discussed earlier. For additional shear rheology data, the reader is directed to Figures S3 and S4 in the supplemental section. Along with the time sweeps, temperature ramp measurements were also performed to further investigate the degradation behavior of the linear, branched, and hyper-branched PC in the presence of air and nitrogen. In those experiments, similar rapid increase in the storage modulus, G', was observed beyond a temperature of $T = 380$ °C in the presence of air for the case of linear and branched PC. Whereas, in the presence of nitrogen, no upturn in the storage modulus was observed until a temperature of $T = 420$ °C. This difference clearly shows the higher rate of degradation that the polymer experience in the presence of oxygen, which leads to earlier degradation as compared to that in the presence of nitrogen. While for the case of hyper-branched, deviation of the storage modulus was observed 30 °C and 70 °C prior to that of the linear and the branched PC in the presence of air and nitrogen respectively.

Extensional rheology

Linear polycarbonate

In Fig. 7, the extensional viscosity, η_E, is plotted as a function of the Hencky strain, ε, for the linear PC for temperatures ranging from $T = 260\,^{\circ}$C to $T = 370\,^{\circ}$C in air (Fig. 7a) and in nitrogen (Fig. 7b). All experiments were performed in the presence of either air or nitrogen for the entirety of the heating cycle and the stretch. The heating resulted in a temperature rise of 4 °C/min. In the experiments presented in Fig. 7, the stretch was performed as soon as the temperature reached the design temperature with no additional time delay. For temperature below $T = 300\,^{\circ}$C in air, the shear rheology measurements suggest that no significant scission or cross-linking of the PC should be observed. As anticipated, at these temperatures, the extensional viscosity was found to decrease with temperature while maintaining a nearly constant Trouton ratios, $Tr = \eta_E(T)/\eta_0(T)$, right around the Newtonian limit of $Tr = 3$ at small strains with only a modest amount of strain hardening at high strains. As described in the introduction, extensional viscosity plays a large role in the dynamics of dripping and the breakup of filaments into drops. As the extensional viscosity decreases with temperature, the result is a decrease in the time needed for the filament to breakup. Under air, the breakup time reduced from 780 to 310 s as the temperature increased from $T = 260$ to $300\,^{\circ}$C.

As seen in Fig. 7a, a decrease in extensional viscosity of 50% was observed with a temperature increase in air from $T = 300$ to $330\,^{\circ}$C. Although the decrease is significant, some decrease is expected as time-temperature superposition (TTS) predicts a reduction in the extensional viscosity of 66–70% across that same temperature range. This suggests that, from $T = 300$ to $330\,^{\circ}$C, a modest amount of molecular structure buildup is occurring. This buildup in molecular structure becomes more and more significant as the temperature was increased. At $T = 340\,^{\circ}$C in air, the extensional viscosity of the linear PC in Fig. 7a, a change in the extensional rheological behavior was observed. At this temperature, the extensional viscosity was found to increase by a factor of four over the course of the experiment, surpassing the viscosity of the linear PC at much lower temperatures. Increasing the temperature further to $T = 350\,^{\circ}$C resulted in a divergence in the extensional viscosity with increasing time at a strain of $\varepsilon = 8$. With further increases in temperature, the extensional viscosity was found to diverge at earlier times and smaller strains.

In order to compare the data for air and nitrogen experiments more clearly, the Trouton ratio for experiments performed at temperatures between $T = 260$ and $340\,^{\circ}$C under both inert and oxygen-rich environment are presented in Fig. 8. By normalizing the extensional viscosity as the Trouton ratio, one can account for reversible temperature-dependent changes to the shear and extensional viscosity associated with the principle of time-temperature superposition. At $T = 260\,^{\circ}$C, the Trouton ratio of both the linear PC stretched in air and nitrogen are similar. However, with increasing strain and time at temperature, the linear PC samples under nitrogen were found to cross-link more rapidly resulting in an extensional viscosity and Trouton ratio roughly 50% larger than the sample under air. At $T = 300\,^{\circ}$C, the initial low-strain Trouton ratio under nitrogen was found to be $Tr = 7$, while in air, the Trouton ratio was found to be $Tr = 5$. This indicates that temperature-induced molecular structure changes had begun during the heating process as the polymer was brought to 300 °C. By increasing the temperature further

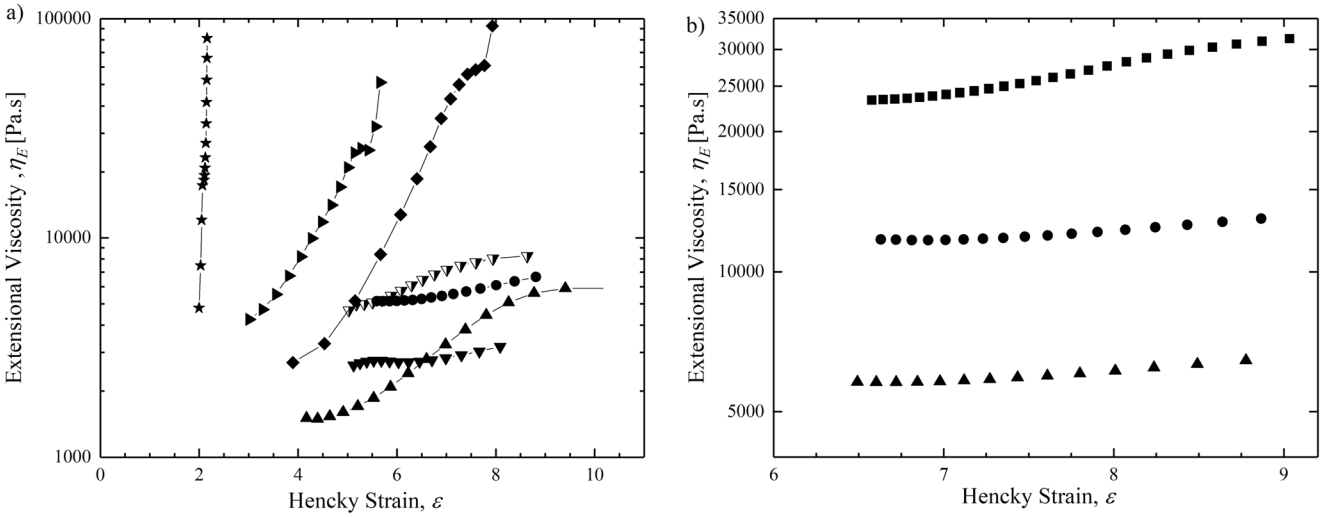

Fig. 7 **a** Capillary breakup extensional rheology measurement of extensional viscosity, η_E, as a function of Hencky strain, ε, for **a** the linear polycarbonate in air and **b** in nitrogen at temperatures $T = 260$ °C (black square), $T = 280$ °C (down-pointing triangle with right half black), $T = 300$ °C (black circle), $T = 330$ °C (black down-pointing triangle), $T = 340$ °C (black up-pointing triangle), $T = 350$ °C (black diamond suit), $T = 360$ °C (black right-pointing pointer), and $T = 370$ °C (black star)

to $T = 340$°C, the low-strain Trouton ratio in nitrogen was found to grow to roughly $Tr = 13$, while remaining close to $Tr = 3$ under air. In this case, the differences between the response of the linear PC under air and nitrogen is nearly a factor of five at small strains. As was observed at 300 ° C, under air, there is a gradual buildup of Trouton ratio over time and strain. However, the growth rate is much faster for the 340 ° C case in air as the Trouton ratio at large strains approaches, but does not quite reach that of the linear PC under nitrogen.

The temperature at which the buildup in the extensional viscosity is observed will be referred to as the transition temperature. This buildup in the extensional viscosity is likely due to temperature-induced cross-linking of the linear PC chains. In fact, if one inspects the extensional viscosity data in Fig. 7a for temperatures beyond 340 ° C, one observes a dramatic increase in extensional viscosity with increasing temperature under air. Initially, at $T = 350$ ° C, the extensional viscosity starts at $\eta_E = 3000$Pa. s and Trouton ratio of $Tr = 4$.

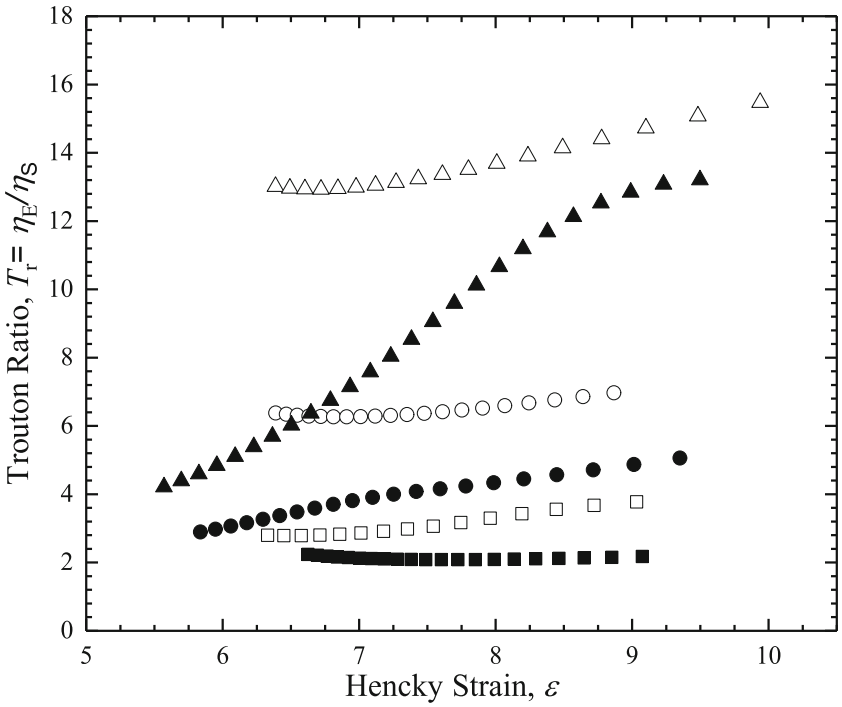

Fig. 8 Comparison of Trouton ratio, *Tr*, of linear polycarbonate in air and nitrogen at temperatures $T = 260$ °C (white square), $T = 300$ °C (white circle), and $T = 340$ °C (white up-pointing triangle). Filled symbols refer to experiments done under air and hollow symbols under nitrogen

However, as the temperature was increased, the extensional viscosity was found to diverge as the filament stopped draining and solidified. This divergence occurred at a smaller imposed strain as the test temperature was increased. The net result was a dramatically increased time for filament breakup, which in these extreme cases was found to diverge to infinity. This massive buildup of molecular structure and the resulting growth in extensional viscosity would clearly improve the performance of the linear PC exposed to a flame as it would eliminate dripping that could feed the flame.

From the literature, it has been shown that the thermal degradation of polycarbonate in nitrogen appears to occur through one initial fast major degradation step and then two minor slow degradations steps. While, under air, an additional minor subsequent slow degradation step has been observed (Li and Huang 1999). The decomposition of PC is initiated by chain scission of the polymer at the weak $O-CO_2$ group. This chain scission results in the reduced molecular weight of the PC and in the extensional viscosity. No degradation is generally seen until a temperature of $T = 300\,^{\circ}$C. Cross-linking has been shown to take place at higher temperatures and it is a process that generally occurs after some stripping of the substituents and involves the creation of bonds between two adjacent polymer chains (Beyler and Hirschler 2002). This process is very important in the formation of chars, since it generates a structure with a higher molecular weight that is less easily volatilized. As seen by our experiments, cross-linking also dramatically increases the extensional viscosity of the polymer melts thus resisting dripping.

In our experiments, the basic structural difference among PCs used is the type of branching which has been influenced by the type of branching agents used to synthesize them. This significantly changes the viscoelastic behavior due to the intrinsic intermolecular entanglements in polymers. Unfortunately, degree of branching is not evident from Fourier transform-infrared spectroscopy (FTIR) analysis. That being said, FTIR analysis is still a strong tool to investigate the changes in the chemical structure of PCs upon thermal degradation in oxygen and nitrogen flow environment (Carroccio et al. 2002; Jang and Wilkie 2004; McNeill and Rincon 1991; Montaudo and Puglisi 1992; Oba et al. 2000). Here, we discuss data from a series of FTIR measurements performed on both neat and heat-treated linear, branched, and hyper-branched PC to gain more insight into the extensional viscosity change in the PC samples. The raw FTIR data can be found in the Supplementary Figures S5 through S8. From these FTIR measurements, a characteristic peak at 1770 cm^{-1} was observed in all neat samples which can be attributed to the infrared absorption from the stretching vibration of C=O of the ester group in polycarbonates. In addition, peaks at 1603 and 1504 cm^{-1} corresponding to the stretching vibrations of C–C bond in the phenylene group in benzene ring were observed. Important to note that change in peak position for C=O or C–O and appearance of new peaks would be evident if there is any significant influence of heat treatment in oxygen or nitrogen on PCs. Following heat treatment at $T = 360\,^{\circ}$C under air, the FTIR spectra of the linear PC were found to contain new peaks at 1656, 1705, and 1728 cm^{-1} which correspond to the C=O vibrations of hydrogen bonded ester groups (Jang and Wilkie 2004; Pretsch et al. 2000). In addition, the appearance of a broad peak at 3330 cm^{-1} gives evidence of an –OH group which is likely hydrogen bonded to C=O group. This broad peak is an indication of cross-linking of linear chains in PC. This explains the reason for substantial increase in extensional viscosity at $T = 360\,^{\circ}$C in the presence of O_2 while such change cannot be observed for samples treated under N_2 environment. Similar structural changes were observed for branched and hyper-branched PC after heat treatment at $T = 320\,^{\circ}$C in the presence of air.

In Fig. 9, the extensional viscosity of linear PC at $T = 340\,^{\circ}$C in air is plotted as a function of the time delay, t_{delay}, imposed after the oven reached the desired experimental temperature and before commencing the stretch. This figure shows the evolution of extensional viscosity as a function of time and reinforces the importance of experimental protocol as time at temperature can have a dramatic effect on the extensional viscosity. During stretch following a delay time of $t = 0$ s, an increase in extensional viscosity can be seen with strain in Fig. 9a, or equivalently, with time in Fig. 9b. This increase is due to the buildup of molecular structure over the period time needed for the capillary bridge to breakup. In this experiment, the breakup takes 75 s. The fact that the extensional viscosity reaches a steady-state value and does not diverge suggests that, although drainage is inhibited, there has not been enough time to fully cross-link or char the sample significantly enough to stop drainage completely. After a delay of $t_{delay} = 150$s, the extensional viscosity was found to diverge rather than reaching a steady state due to the considerable cross-linking that has taken place while being held at 340 °C. This can also be seen with the increase in the extensional viscosity at low strains. As the delay time for stretch was increased further, the extensional viscosity was found to diverge at smaller and smaller strains. It would be convenient to find a way to collapse all these data onto a single master curve by plotting the extensional viscosity against time at temperature for instance rather than strain. In these experiments, strain is equivalent to $\varepsilon = \dot{\varepsilon}t$ so the time of the stretch can be found from $t_{flow} = \varepsilon/\dot{\varepsilon}$. Unfortunately as seen in Fig. 9b, this does not result in the anticipated master curve as the kinematics of the extensional flow appear to also play a role in the rate of cross-linking. As a result, the delay time is not precisely equivalent to the flow time with respect to reaction kinetics. This could be because the

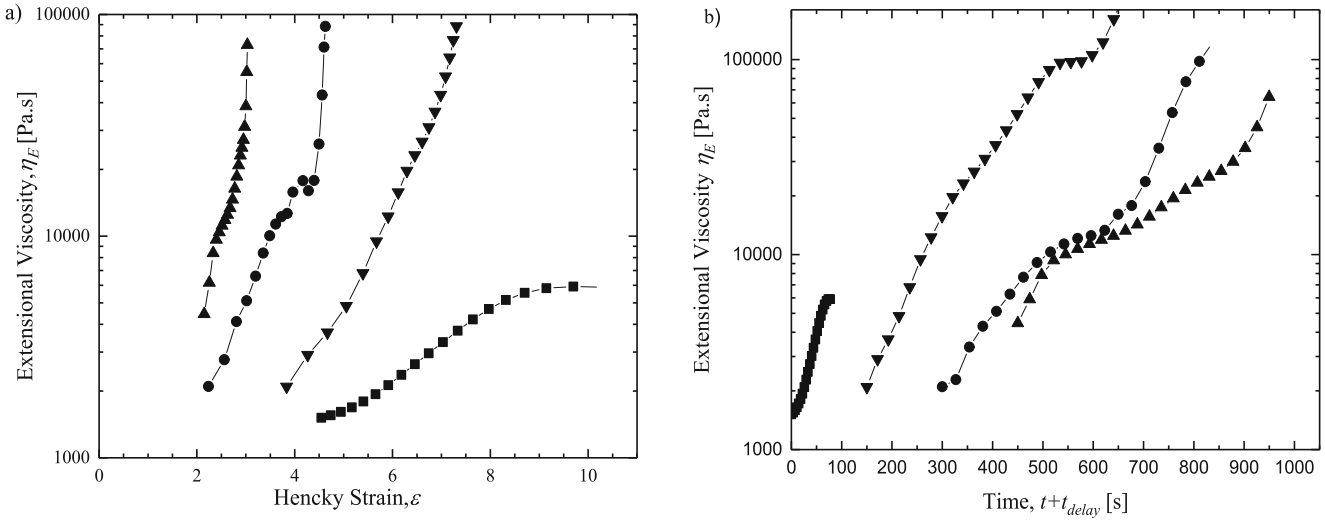

Fig. 9 Plot of **a** extensional viscosity of linear polycarbonate at temperature $T = 340$ °C as a function of Hencky strain and **b** time at the experimental temperature which includes a delay time imposed before the onset of stretch. This data include experiments with a delay time after the experimental temperature was reached with a delay time of $t_{\text{delay}} = 0$ s (black square), 150 s (black down-pointing triangle), 300 s (black circle), and 450 s (black up-pointing triangle). All experiments were performed in air

imposed flow changes the filament geometry, increasing the surface area and exposing more material to the environment or it could be because the stretching flow deforms the chains in the polymer melt allowing for more cross-linking opportunities.

Branched polycarbonate

In Fig. 10, the extensional viscosity of the branched PC is plotted as a function of Hencky strain for temperature ranging from $T = 280$ ° C to $T = 370$ ° C in air (Fig. 10a) and in nitrogen (Fig. 10b). The same experimental protocol used for the linear PC measurement was followed here. For temperature below $T < 300$ ° C, no obvious sign of polymer degradation was observed. For those temperatures, the extensional viscosity was found to decay with temperature following TTS and under air, a constant Trouton ratio of $Tr = 3$ was found. As the temperature was increased from $T = 300$ ° C to $T = 320$ ° C, an increase in the extensional viscosity with strain and time similar to that observed for the linear PC case was observed due to buildup of molecular structure either through cross-linking or branching. The Trouton ratios are compared for the branched PC experiments performed in Fig. 11. A closer inspection of the data in Fig. 11 shows that at $T = 300$ ° C, the calculated

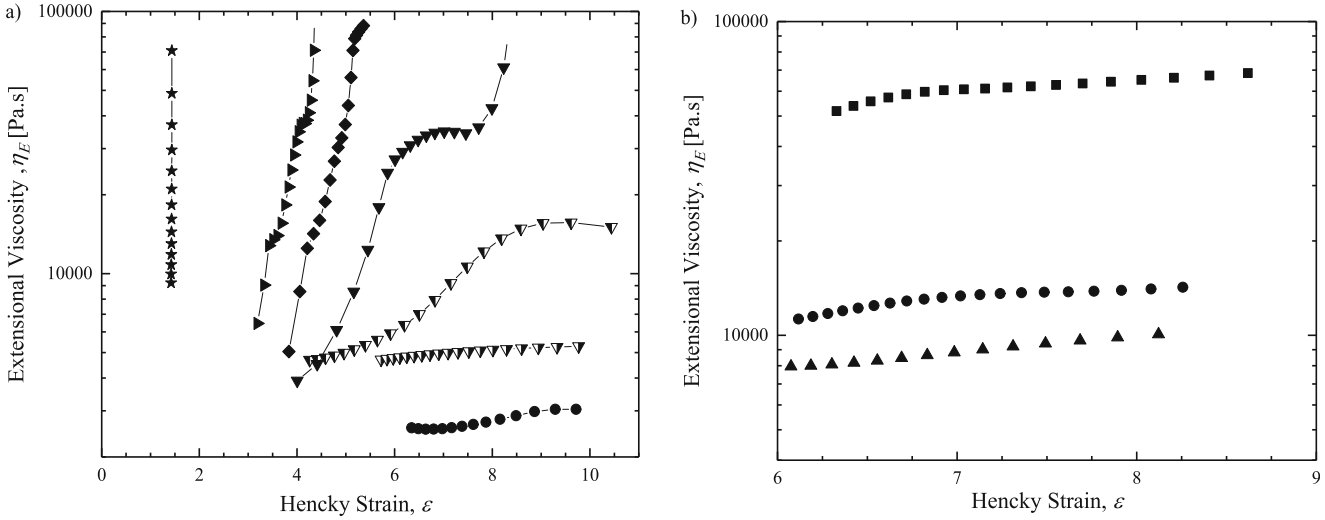

Fig. 10 **a** Capillary breakup extensional rheology measurement of extensional viscosity, η_E as a function of Hencky strain, ε, for **a** the branched polycarbonate in air and **b** in nitrogen at temperatures $T =$ 260 °C (black sqaure), $T = 280$ °C (down-pointing triangle with right half black), $T = 300$ °C (black circle), $T = 320$ °C (down-pointing triangle with left half black), $T = 330$ °C (black down-pointing triangle), $T = 340$ °C (black up-pointing triangle), $T = 350$ °C (black diamond suit), $T = 360$ °C (black right-pointing pointer), $T = 370$ °C (black star)

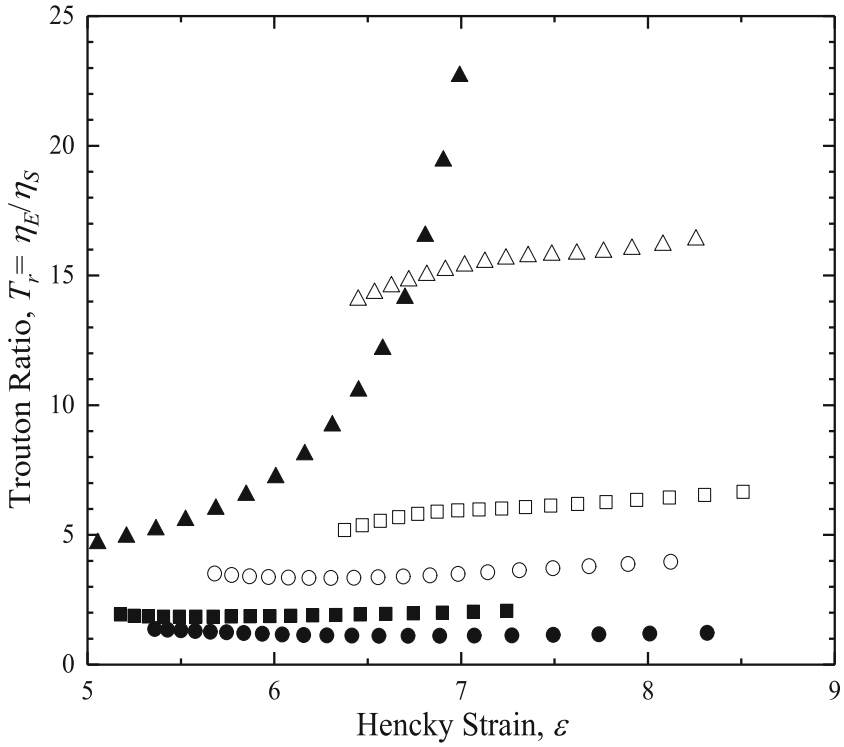

Fig. 11 Comparison of Trouton ratio, *Tr*, of branched polycarbonate in air and nitrogen at temperatures $T = 260$ °C (white square), $T = 300$ °C (white circle), and $T = 340$ °C (white up-pointing triangle). Filled symbols refers to experiments done under air and hollow symbols under nitrogen

Trouton ratio under nitrogen was found to be $Tr = 4$ while under air the Trouton ratio was $Tr = 1$. The larger Trouton ratio under nitrogen suggests that the branched PC in air had experienced some thermal degradation under air likely the result of chain scission or perhaps the loss of branches along the backbone. The branched PC appears to be more sensitive to polymer degradation than the linear PC. This threefold reduction in the extensional viscosity and Trouton ratio in air is 60% larger than the reduction observed at these temperatures for the case of the linear PC. As for the experiments performed at $T = 320$ ° C, at lower strains, the extensional viscosity under air starts at a value one-third that under nitrogen, but then recovers a significant amount of the extensional viscosity with increasing strains and time at temperature. Compared to the linear PC, significant cross-linking appears to happen at much lower temperatures for the branched PC samples. For instance, the divergence in the extensional viscosity observed in Fig. 10a was found to occur at a transition temperature of $T = 330$ ° C for the branched PC samples in air, but not until $T = 350$ ° C for the linear PC case. This could be due in part to the increase in the number of chain end in the branched case or due to the presence of some unused branching agent remaining in the sample. It is important to note that the divergence in the extensional viscosity is only observed for samples under air for both the linear and branched PC melts. Beyond the temperature $T = 330$ ° C in air, the growth rate of the extensional viscosity with strain accelerated with increasing temperature. This growth rate is clearly visible from Figs. 10 and 11. For instance, if one compares the early strain Trouton ratio at temperature $T = 340$ ° C under air to that under nitrogen, one finds a Trouton ratio of $Tr = 5$ and $Tr = 15$ respectively. As the strain was increased, the Trouton ratio under nitrogen was found to remain essentially constant. However, under air, the Trouton ratio was found to quickly grow to $Tr = 25$ at a strain of $\varepsilon = 7$. This dramatic increase in the extensional viscosity resulted in an increased time for filament breakup of the branched PC in air compared to the linear PC. It is therefore expected that the branched PC will provide better flame resistance than the linear PC when exposed to a high-temperature heat source like a flame.

In Fig. 12, the extensional viscosity of branched PC at $T = 340$ ° C in air is plotted as a function of delay time imposed after the oven reached the desired temperature and before beginning the stretch. During the stretch following a delay time of $t_{delay} = 0$ s, an increase in extensional viscosity can be seen with strain in Fig. 12a and with time in Fig. 12b. The extensional viscosity was found to reach a plateau at larger strains before diverging at $t = 120$ s. With increasing delay time, the divergence of the viscosity was found to occur at earlier and earlier strains. As before, the data was not found to collapse if replotted versus total time at temperature as seen in Fig. 12. However, when compared to the linear PC, the branched PC was found to be even more sensitive to time at temperature as the filament solidified more quickly.

Hyper-branched polycarbonate

In Fig. 13, the extensional viscosity of the hyper-branched PC is plotted as a function of Hencky strain for temperature

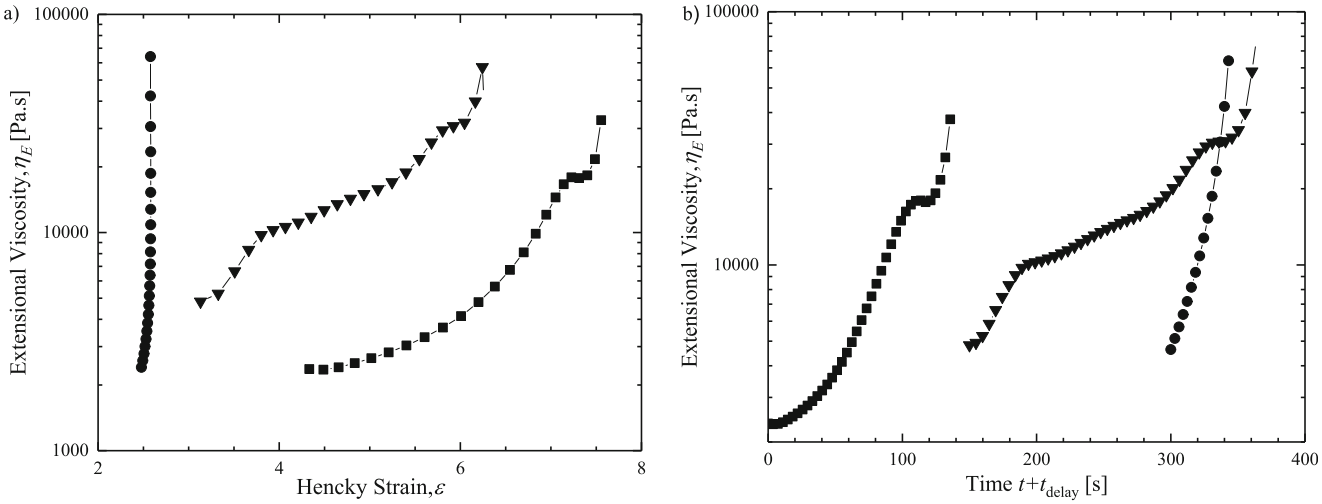

Fig. 12 Plot of **a** extensional viscosity of branched polycarbonate at temperature $T = 340$ °C as a function of Hencky strain and **b** time at the experimental temperature which includes a delay time imposed before the onset of stretch. This data include experiments with a delay time after the experimental temperature was reached with a delay time of $t_{delay} = 0$ s (black square), 150 s (black down-pointing triangle), and 300 s (black circle). All experiments were performed in air

ranging from $T = 250$ ° C to $T = 350$ ° C in air (Fig. 13a) and nitrogen (Fig. 13b). As the temperature was increased from $T = 250$ ° C to $T = 280$ ° C in air, no significant molecular changes were observed. The Trouton ratio remained constant at $Tr = 14$ across the entire temperature range. With a further increase in the temperature to $T = 300$ ° C, an increase in extensional viscosity was observed with increasing strain. Under air, the transition temperature at which the extensional viscosity was found to diverge was even lower than for the branched PC; $T_t = 320$ ° C versus 330 ° C. Additionally, as seen in Fig. 13b, it appears that, for the hyper-branched PC, the presence of air actually inhibits buildup of molecular structure. Under nitrogen, the transition temperature drops from $T_t =$ 320 ° C in air to $T_t = 280$ ° C. These trends are opposite to those observed for the linear and branched PC where the presence of air was necessary to initiate significant polymer cross-linking at elevated temperatures. In the previous cases, the data did not diverge under nitrogen in any of the tests that were performed. This observation demonstrates the importance that the number or chemistry of the polymer end group can play in flame resistance. The linear and branched PC samples had end groups composed of the ester group, while the hyper-branched PC had HBN end groups. The activity of these end groups appears to be suppressed by the presence of oxygen. Above a flame, the gas is often devoid of air as it has been depleted by the flame and replaced with various products of combustion. Having a material that can heavily cross-link in the absence of air may be critical to the flame-resistant

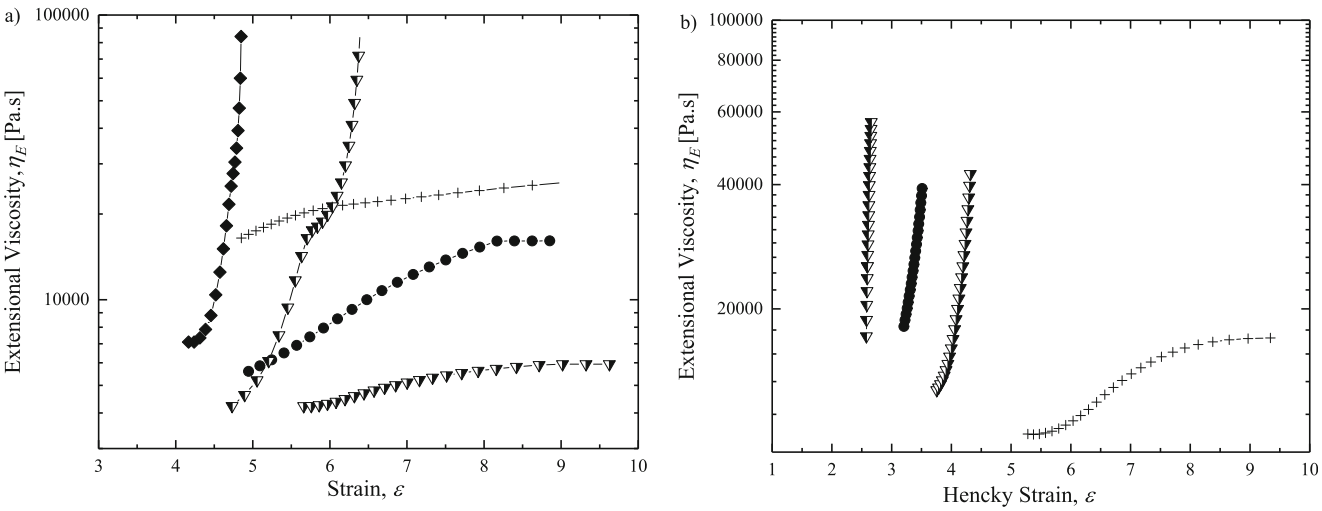

Fig. 13 **a** Capillary breakup extensional rheology measurements of extensional viscosity, η_E as a function of Hencky strain, ε, for **a** the hyper-branched polycarbonate in air and **b** in nitrogen at temperatures $T = 250$ °C (plus sign), $T = 280$ °C (down-pointing triangle with right half black), $T = 300$ °C (black circle), $T = 320$ °C (down-pointing triangle with left half black), $T = 350$ °C (black diamond suit)

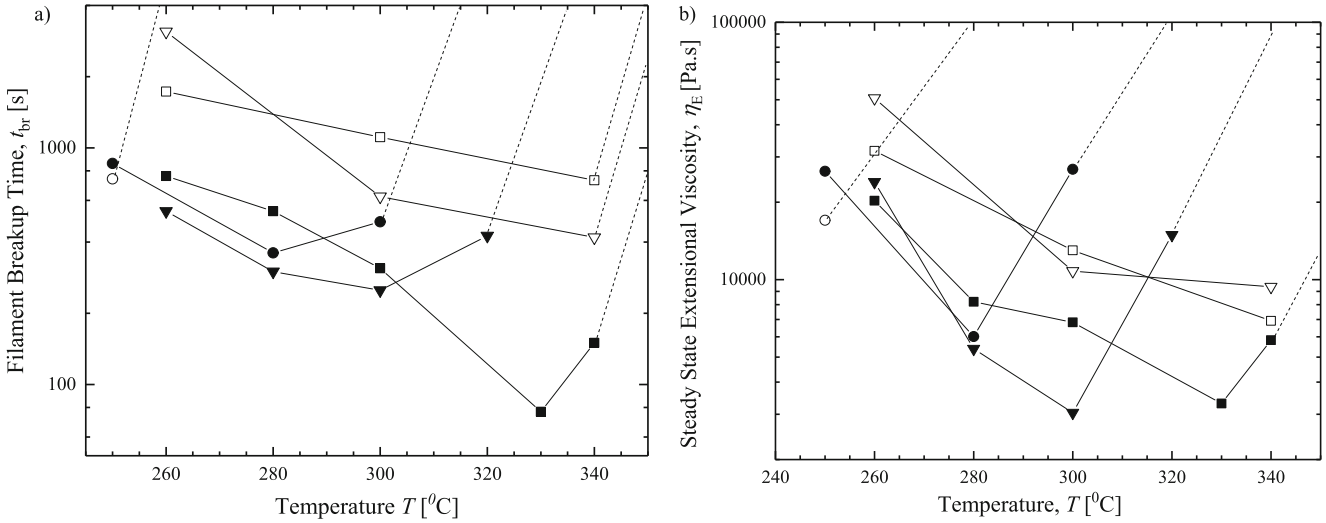

Fig. 14 **a** Plot of breakup time, t_{br}, and **b** steady-state extensional viscosity, η_E, as a function of temperature, T, for linear (black square), branched (black down-pointing triangle), and hyper-branched (black circle) polycarbonate. Filled symbols correspond to experiment in air while hollow symbols correspond to nitrogen. The dashed lines show the point of divergence when the filament solidifies

performance when exposed to a flame. For the hyper-branched PC, the divergence of η_E at low temperatures is highly desirable.

Filament breakup time and steady-state extensional viscosity

In Fig. 14a, plot of the filament breakup time, t_{br}, is plotted against temperature for the linear, branched, and hyper-branched PC under air and nitrogen. Take for example the case of the linear PC in air. The breakup time was initially found to be $t_{br} = 780$ s at $T = 260$ ° C, with increasing temperature, the breakup time was found to decrease until it reached a minimum of $t_{br} = 80$ s at $T = 330$ ° C. This initial decrease is due primarily to the reduction in viscosity expected from time-temperature superposition but may also include effects of some modest degradation of the polymer chains at these moderate temperatures. This can also be seen from the data in Fig. 14b, where the steady-state extensional viscosity decreased from $\eta_E = 22,000$ Pa s at $T = 260$ ° C to $\eta_E = 3500$ Pa s at $T = 330$ ° C. As the temperature increased further, the breakup time increased to $t_{br} = 160$ s at $T = 340$ ° C before diverging at higher temperature because of significant cross-linking resulting in a divergence of the extensional viscosity as seen in Fig. 14b. At that point, the filament diameter was found to stop decaying and the breakup time diverged to infinity as the filament solidified. The minimum breakup time under air was found to increase from $t_{br} = 80$ s to 250 s and finally to 360 s as the degree of polymer branching was increased. Under nitrogen, the minimum breakup time for the hyper-branched case was nearly 1000 s. Conversely, the breakup time under nitrogen at moderate temperatures was only a factor of two or three higher for both linear and branched PC as compared to the breakup time in air. However, the divergence of the extensional viscosity under air suggests that in these cases, the presence of oxygen would make these polymers more flame resistant at higher temperatures.

Conclusion

The variation in the extensional viscosity of three selected commercially available linear, branched, and hyper-branched polycarbonates was studied using a newly designed high-temperature capillary breakup extensional rheometer (CaBER). Extensional rheology measurements were performed at temperatures varying from $T = 250$ to 370 ° C in both an inert and an oxygen-rich environment for all three polycarbonates. The design of the CaBER oven allowed us to make measurements under condition where polymer degradation was either expected or not. The goal of these experiments was to use extensional rheology to better understand the behavior of polymers like polycarbonate when they are exposed to a high-temperature heat source like a flame. Under these extreme conditions, the determination of whether a polymer is flame resistant or not depends largely on whether or not the molten polymer drips and feeds the fire. As the formation and release of a drip is a process dominated by an extensional flow, it was our hypothesis that characterization of the evolution of a polymer's extensional viscosity with time and temperature under extreme conditions can be a sensitive probe of changes to a polymer's chemical architecture and a powerful new tool for predicting the polymer's behavior when exposed to a flame.

At the low end of the temperature range studied, no degradation of the linear and branched PC was observed in the shear rheology measurements. However, the extensional rheology measurements showed evidence of a modest amount of chain scission under air which was found to reduce the Trouton ratio of the polycarbonate by 10 or 15%. The branched PC was found to be more sensitive to chain scission than the linear PC. At higher temperatures, beyond $T > 300\,^{\circ}\mathrm{C}$, significant increases in the extensional viscosity of the three different PCs were observed resulting from changes to the molecular structure of the PC. These changes to the molecular structure are likely the result of polymer cross-linking or increased branching of the polymer chain at high temperatures. In all cases, the rate of growth in the extensional viscosity was found to increase with both temperature and time at temperature. In the case of the linear and branched PC, the largest changes to the extensional viscosity were observed in the presence of air. For the hyper-branched case, however, changes to the molecular structure of the PC were found to occur more quickly under nitrogen resulting in large extensional viscosity growth. Under air, at extremely high temperatures, the extensional viscosity of all three polycarbonates was found to diverge to infinity which ultimately resulted in the cessation of the filament drainage as the polymer melt became so heavily cross-linked that it essentially solidified. In some cases, the polymer would blacken and form a char. For the hyper-branched PC, the presence of air had an inhibiting effect on polymer cross-linking. However, due to the presence of the polymer end group used to enhance branching, the buildup of molecular structure was found to be even more rapid in the presence of nitrogen than either the linear or the branched PC in air. In fact, for both the linear and the branched PC, the extensional viscosity was not found to diverge under nitrogen even at 370 °C. For comparison, the extensional viscosity of the hyper-branched PC was found to diverge under nitrogen at just 280 °C.

This temperature-induced cross-linking and increase in the extensional viscosity of the PC can improve the flame-resistant properties of the polycarbonate by slowing and even restricting dripping from polymeric components near high heat surges. In many cases, the regions of high heat near an open flame are also devoid of oxygen. As a result, the divergence of the hyper-branched PC under nitrogen might be a distinct advantage and a feature that could be incorporated when designing and testing other flame-resistant polymers. Finally, it should be noted that with these experiments, we have demonstrated measurement of the extensional viscosity was found to be several orders of magnitude more sensitive to temperature-induced changes to the molecular structure than measurements of shear rheology.

Acknowledgments The authors would like to thank Christian Clasen of KU Leuven for the use of his Edgehog software, Zachary Anderson (SABIC) for his Shear rheology measurements, and M. D. Arifur Rahman (University of Massachusetts, Amherst) for the FTIR analysis.

Funding information

This research received funding from SABIC.

References

Anna SL, McKinley GH (2001) Elasto-capillary thinning and breakup of model elastic liquids. J Rheol 45:115–138

Bach A, Rasmussen HK, Hassager O (2003) Extensional viscosity for polymer melts measured in the filament stretching rheometer. J Rheol 47:429–441

Bazilevsky AV, Entov VM, Rozhkov AN. (1990) Liquid filament microrheometer and some of its applications. In: Oliver DR (ed) Proc. Third European Rheology Conference, Edinburgh. pp 41–43

Beyler CL, Hirschler MM (2002) Thermal decomposition of polymers SFPE handbook of fire protection engineering 2:32

Bischoff White E, Rothstein JP (2012) Extensional flow-induced crystallization of polypropylene. Rheol Acta 51:303–314

Carroccio S, Puglisi C, Montaudo G (2002) Mechanisms of thermal oxidation of poly (bisphenol a carbonate). Macromolecules 35:4297–4305

Chellamuthu M, Arora D, Winter HH, Rothstein JP (2011) Extensional flow-induced crystallization of isotactic poly(1-butene). J Rheol 55:901–920

Clasen C, Phillips PM, Palangetic L, Vermant J (2012) Dispensing of rheologically complex fluids: the map of misery. AICHE J 58:3242–3255

Clasen C, Plog JP, Kulicke WM, Owens M, Macosko C, Scriven LE, Verani M, McKinley GH (2006) How dilute are dilute solutions in extensional flows? J Rheol 50:849–881

DeMaio V, Dong D, Gupta A (2000) Using branched polypropylene as a melt strength modifier-improvement in sheet sag resistance (236). In: Technical papers of the annual technical conference-society of plastics engineers incorporated. pp 799–803

Entov VM, Hinch EJ (1997) Effect of a spectrum of relaxation times on the capillary thinning of a filament of elastic liquid. J Non-Newtonian Fluid Mech 72:31–53

Filippone G, Carroccio S, Curcuruto G, Passaglia E, Gambarotti C, Dintcheva NT (2015) Time-resolved rheology as a tool to monitor the progress of polymer degradation in the melt state–part II: thermal and thermo-oxidative degradation of polyamide 11/organo-clay nanocomposites. Polymer 73:102–110

He C, Costeux S, Wood-Adams P (2004) A technique to infer structural information for low level long chain branched polyethylenes. Polymer 45:3747–3754

Jang BN, Wilkie CA (2004) A TGA/FTIR and mass spectral study on the thermal degradation of bisphenol A polycarbonate. Polym Degrad Stab 86:419–430

Kandola B, Ndiaye M, Price D (2014) Quantification of polymer degradation during melt dripping of thermoplastic polymers. Polym Degrad Stab 106:16–25

Kandola B, Price D, Milnes G, Da Silva A (2013) Development of a novel experimental technique for quantitative study of melt dripping of thermoplastic polymers. Polym Degrad Stab 98:52–63

Kojic N, Bico J, Clasen C, McKinley GH (2006) Ex vivo rheology of spider silk. J Exp Biol 209:4355–4362

Kruse M, Wagner MH (2016) Time-resolved rheometry of poly (ethylene terephthalate) during thermal and thermo-oxidative degradation. Rheol Acta 55:789–800

Kulicke W-M, Kniewske R (1984) The shear viscosity dependence on concentration, molecular weight, and shear rate of polystyrene solutions. Rheol Acta 23:75–83

Laoutid F, Bonnaud L, Alexandre M, Lopez-Cuesta J-M, Dubois P (2009) New prospects in flame retardant polymer materials: from fundamentals to nanocomposites. Mater Sci Eng R Rep 63:100–125

Li XG, Huang MR (1999) Thermal degradation of bisphenol A polycarbonate by high-resolution thermogravimetry. Polym Int 48:387–391

Matzen M, Kandola B, Huth C, Schartel B (2015) Influence of flame retardants on the melt dripping behaviour of thermoplastic polymers. Materials 8:5621–5646

McKinley GH (2005) Visco-elasto-capillary thinning and break-up of complex fluids. In: Binding DM, Walters K (eds) Annual Rheology Reviews. The British Society of Rheology, Aberystwyth, Wales, UK, pp 1–49

McKinley GH, Tripathi A (2000) How to extract the Newtonian viscosity from capillary breakup measurements in a filament rheometer. J Rheol 44:653–670

McNeill I, Rincon A (1991) Degradation studies of some polyesters and polycarbonates—8. Bisphenol A polycarbonate. Polym Degrad Stab 31:163–180

Montaudo G, Puglisi C (1992) Thermal decomposition processes in bisphenol A polycarbonate. Polym Degrad Stab 37:91–96

Mun RP, Byars JA, Boger DV (1998) The effect of polymer concentration and molecular weight on the break-up of laminar capillary jets. J Non-Newtonian Fluid Mech 74:285–297

Najafi N, Heuzey M-C, Carreau PJ, Therriault D, Park CB (2014) Rheological and foaming behavior of linear and branched polylactides. Rheol Acta 53:779–790

Oba K, Ishida Y, Ito Y, Ohtani H, Tsuge S (2000) Characterization of branching and/or cross-linking structures in polycarbonate by reactive pyrolysis− gas chromatography in the presence of organic alkali. Macromolecules 33:8173–8183

Papageorgiou DT (1995) On the Breakup of Viscous Liquid Threads. Physics of Fluids 7:1529–1544

Plog JP, Kulicke WM, Clasen C (2005) Influence of the molar mass distribution on the elongational behaviour of polymer solutions in capillary breakup. Appl Rheol 15:28–37

Pretsch E, Buehlmann P, Affolter C, Pretsch E, Bhuhlmann P, Affolter C (2000) Structure determination of organic compounds. Springer,

Rayleigh L (1879) On the instability of jets. Proc Lond Math Soc 10:4–13

Renardy M (1995) A numerical study of the asymptotic evolution and breakup of Newtonian and viscoelastic jets. J Non-Newtonian Fluid Mech 59:267–282

Rodd LE, Scott TP, Cooper-White JJ, McKinley GH (2005) Capillary break-up rheometry of low-viscosity elastic fluids. Appl Rheol 15:12–27

Salehiyan R, Malwela T, Ray SS (2017) Thermo-oxidative degradation study of melt-processed polyethylene and its blend with polyamide using time-resolved rheometry. Polym Degrad Stab 139:130–137

Shangguan Y, Zhang C, Xie Y, Chen R, Jin L, Zheng Q (2010) Study on degradation and crosslinking of impact polypropylene copolymer by dynamic rheological measurement. Polymer 51:500–506

Stelter M, Brenn G, Yarin AL, Singh RP, Durst F (2000) Validation and application of a novel elongational device for polymer solutions. J Rheol 44:595–616

Stone HA (1994) Dynamics of drop deformation and breakup in viscous fluids. Annu Rev Fluid Mech 26:65–102

Wang Y, Jow J, Su K, Zhang J (2012) Dripping behavior of burning polymers under UL94 vertical test conditions. J Fire Sci 30:477–501

Wang Y, Zhang F, Chen X, Jin Y, Zhang J (2010) Burning and dripping behaviors of polymers under the UL94 vertical burning test conditions fire and materials. An Int J 34:203–215

Winter HH, Chambon F (1986) Analysis of linear viscoelasticity of a crosslinking polymer at the gel point. J Rheol 30:367–382

Yesilata B, Clasen C, McKinley GH (2006) Nonlinear shear and extensional flow dynamics of wormlike surfactant solutions. J Non-Newton Fluid Mech 133:73–90